

***In situ* Vibrational Probes of Epoxy Gelation**

Lérys Granado^{1,2,3*}, Stefan Kempa^{1*}, Laurence John Gregoriades¹, Frank Brüning¹, Anne-Caroline Genix², Jean-Louis Bantignies², Nicole Fréty³ and Eric Anglaret²

¹ Atotech Deutschland GmbH, Erasmusstraße 20, 10553 Berlin, Germany

² L2C, Univ. Montpellier, CNRS, 34095 Montpellier, France

³ ICGM, Univ. Montpellier, CNRS, 34095 Montpellier, France

* Corresponding Authors: lerys.granado@live.fr and stefan.kempa@atotech.com

Total number of figure: 6. Total number of page: 4.

Table of Content

1. Characterization of system (A).....	2
1. Fillers Characterization.....	2
2. Glass transition temperature.....	2
3. Stoichiometry epoxy:hardener (r) by ¹ H NMR.....	2
4. Hardener functionality (f) by MALDI-ToF	3
2. NIR cure monitoring of system (B)	4
3. NIR cure monitoring of system (C).....	4

1. Characterization of system (A)

1. Fillers Characterization

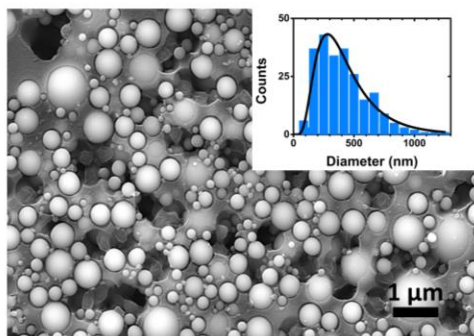


Figure S1. Scanning electron micrograph of the composite surface revealing the glass fillers (secondary electron mode). Inset: filler diameter distribution as determined from image analysis (centered near 300 nm).

2. Glass transition temperature

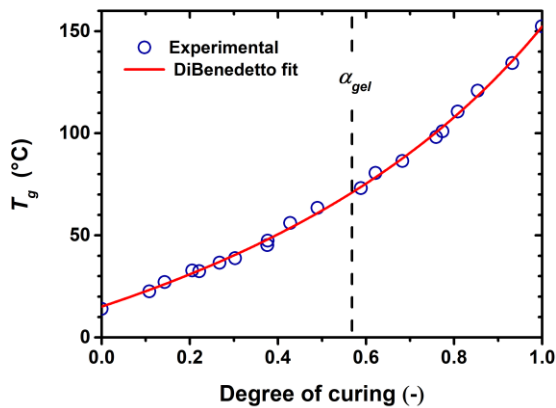


Figure S2. Evolution of the glass transition temperature as a function of the degree of curing, determined using DSC at 10 K/min.

3. Stoichiometry epoxy:hardener (r) by ^1H NMR

The uncured polymer matrix was dissolved in CDCl_3 and filtered, and the NMR spectrum was acquired on a Bruker AC-400 spectrometer. The spectrum of the polymer matrix is displayed in Figure S3. Oxirane protons are observed at 2.6-2.9 ppm (OCH_2) and 3.4-3.5 (OCH). The peaks in the range 3.7-4.5 ppm are assigned to two types of protons: ($-\text{O}-\text{CH}_2$) from the glycidyl moieties of epoxy and ($-\text{CH}_2-$) of methylene bridge of the phenol-formaldehyde hardener. The aromatic protons (6.7-8.3 ppm) count theoretically for 4 protons from bisphenolic epoxy and ca. 3 protons for phenol-formaldehyde oligomers (one OH + 2 CH_2 per aromatic ring, see next Figure). The observed aromatic protons count is 6.89, agreeing with the theoretical count in case of stoichiometric ratio ($= 7$). Thus, we estimate the stoichiometric ratio at $r \sim 1$.

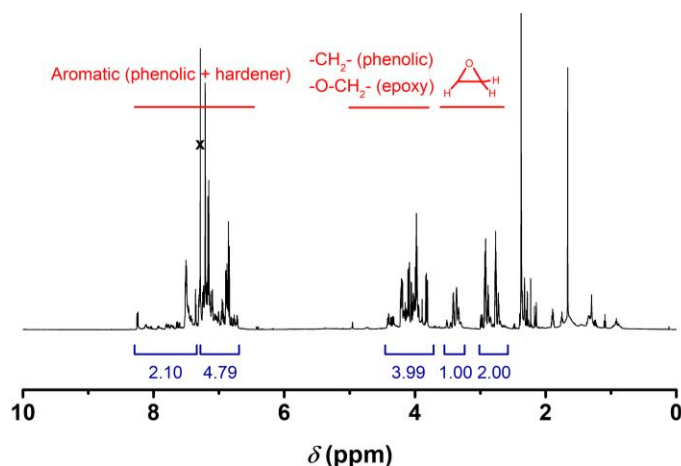


Figure S3. ^1H NMR spectrum of the polymer matrix in CDCl_3 .

4. Hardener functionality (f) by MALDI-ToF

The functionality of the phenol-formaldehyde hardener of system (A) and (B) was investigated by matrix assisted laser desorption/ionization time of flight mass spectrometry (MALDI-ToF). The uncured film was dissolved in acetone and filtered (PTFE 0.22 μm). 2,5-Dihydroxybenzoic acid (DHB) was used as matrix without any cationising agent. Acetone was used as solvent (mixture polymer:DHB solutions, 1:1, v:v; 1 μL was dried on the target plate). The spectrometer was a Bruker Ultraflex ToF/ToF. The laser wavelength was 337 nm, with an irradiation frequency of 100 Hz. The ions were accelerated with a voltage of +25 kV.

Figure S4a shows a typical MALDI-ToF spectrum. Several incrementing units are identified on the mass spectrum, every forming 8 series of peaks. The observed incrementing molecular weight (M_w) of 106.0 ± 0.1 Da perfectly matches with the M_w of phenol-formaldehyde monomer (phenol + methylene bridge). The 2 most relevant series due to their high intensity are highlighted in colors. Series 1 is associated to $(M + \text{CH}_2\text{OH} (\text{end group}) + \text{H}^+)$ adduct and series 2 to $(M + 2 \text{CH}_2\text{OH} (\text{end group}) + \text{DGEBA} + \text{H}^+)$. The discrepancy between theoretical and observed adducts M_w is less than 2 Da. For system (A), the distribution of the hardener functionality is then deduced from series 1, leading to a distribution centered on $f = 4$ (Figure S4b). A very close spectrum was recorded for system (B), therefore the functionality of (B) is considered identical to that of (A).

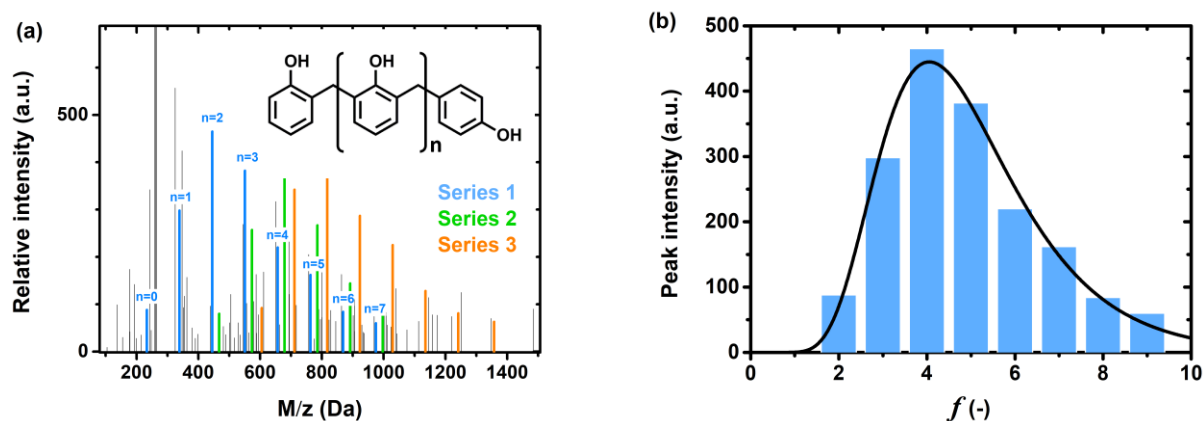


Figure S4. (a) MALDI-ToF spectrum of the system (A), with highlighted relevant series with repetition units of 106.0 Da.

(b) Intensity of series 1 peaks as a function of the functionality of hardener (A), distribution centered on $f=4$.

2. NIR cure monitoring of system (B)

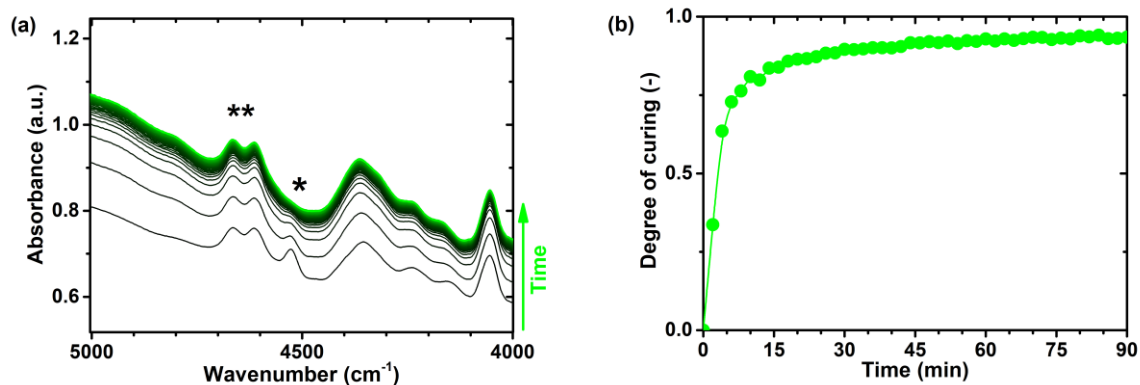


Figure S5. (a) Typical NIR spectra during curing of system (B) at 190 °C. (b) Associated kinetic profile.

3. NIR cure monitoring of system (C)

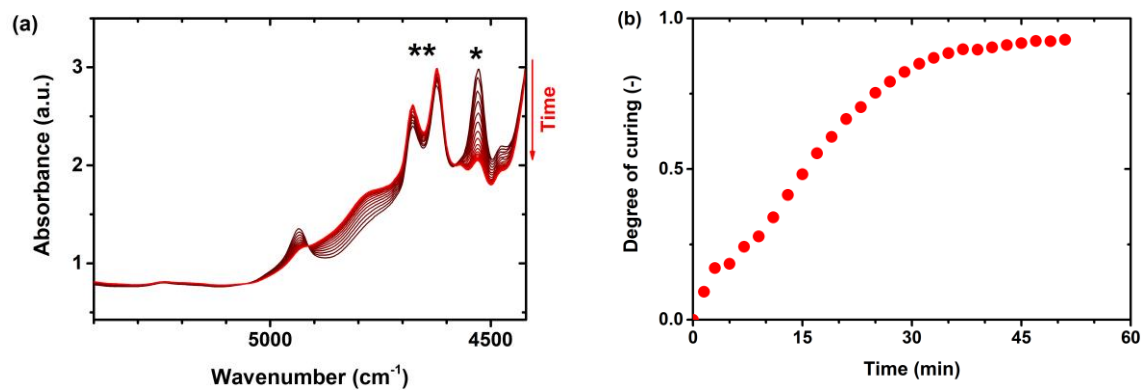


Figure S6. (a) Typical NIR spectra during curing of system (C) at 60 °C. (b) Associated kinetic profile.